4
Multi-Terminal Transmission System

4.1 INTRODUCTION

The importance of a power system includes high reliability and efficiency. Multi-terminal lines play an important role in transmitting the power economically, to cope up with the demand in the present scenario of increased industrialization. The quick fault detection and fault location on these lines help in improving the power quality, reliability and economical operation of power system.

4.2 SYSTEM MODEL AND PARAMETERS

The single line diagram of the system considered, along with various blocks of the proposed scheme, is shown in Figure 4.1. The three-transmission system, under consideration, has a voltage rating of 345kV and operates at a frequency of 50Hz, connecting three AC systems. The parameters of the system under study are presented in Table-4.1 [Ahmadimanesh and Shahrtash, 2013].

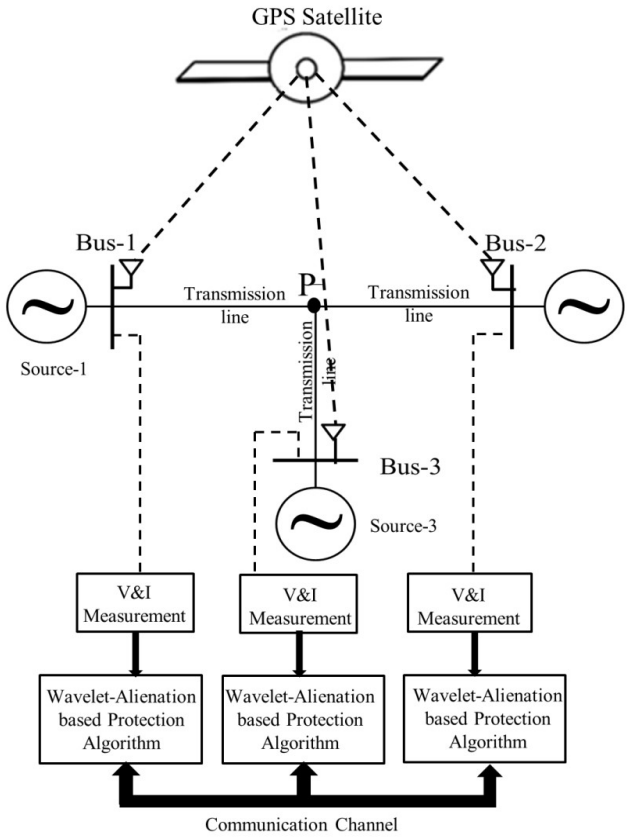

Figure 4.1: Proposed System

4.3 PROPOSED ALGORITHM

The sampling of three-phase voltage and current signals, at all terminals, is carried out at a frequency of 1.6 KHz. The sampling process is synchronized with the help of GPS clock. The three-phase differential current is obtained by adding the respective phase currents from all the terminals. The samples of this differential current of each phase, obtained over a moving window of quarter cycle length, are decomposed with db2 mother wavelet to compute

approximate coefficients. Alienation coefficients are computed by comparing approximate coefficients of current window with those of previous window as shown in Figure 4.2, which is termed as fault index.

Under normal conditions, the value of fault index remains zero since the two successive windows have same set of approximate coefficients. In the event of fault, the approximate coefficients of current window would differ from those of preceding window. Thus, alienation coefficients would increase from zero to a finite value, indicating fault. Thus fault index is compared with a threshold **(0.07)** value to detect the fault in a phase. Thus, the fault index of faulty phase/s would have greater value than the threshold whereas that of healthy phase/s would be lower than the threshold. The flow chart for fault detection and classification is given in Figure 4.2 and flow chart for faulty section identification and fault location is given in Figure 4.3.

Table 4.1: Three-Terminal Transmission System Parameters

Source Voltage (kV)		V_1	V_2	V_3
		$345 \angle 20^0$	$345 \angle 0^0$	$345 \angle 10^0$
Source Imp. (Ω)	Positive Sequence	Z_{11}	Z_{21}	Z_{31}
		0.091+j2.598	0.091+j2.598	0.091+j2.598
	Zero Sequence	Z_{10}	Z_{20}	Z_{30}
		0.878+j4.515	0.878+j4.515	0.878+j4.515
Line Imp. (Ω/km)	Positive Sequence	0.0756+ j0.4235		
	Zero Sequence	0.4549+ j1.223		
Line Lengths (km)		1-P Section	2-P Section	3-P Section
		150	100	80

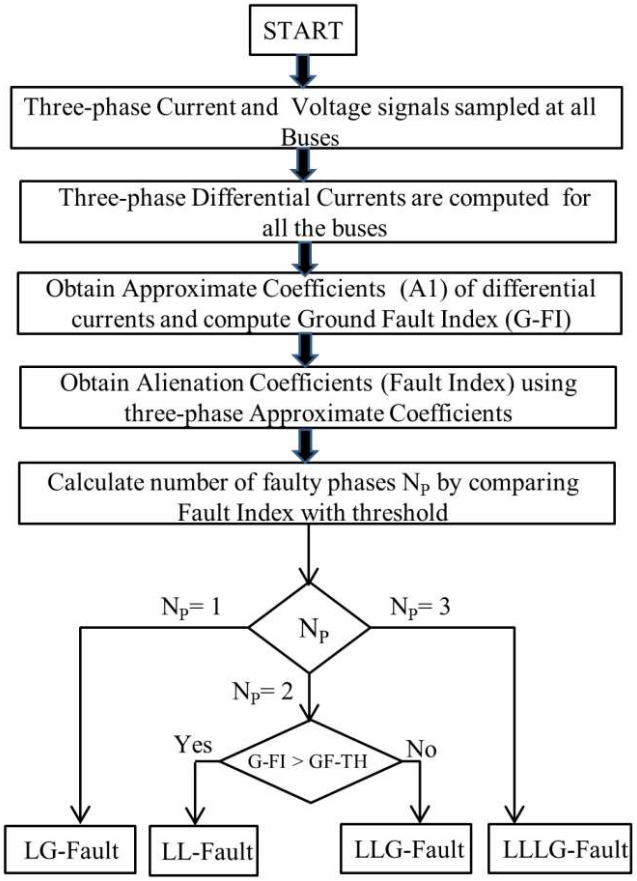

Figure 4.2: Flowchart for fault detection and classification

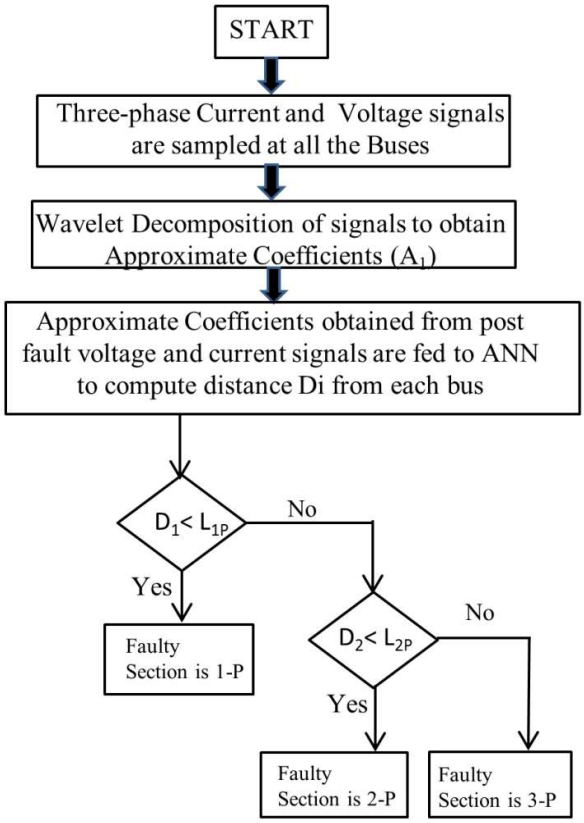

Figure 4.3: Flowchart for Fault Location and Faulty Section Identification

4.4 DETECTION AND CLASSIFICATION OF FAULTS

The proposed algorithm is demonstrated in Figure 4.4, by simulating AG fault at 75km from bus-1. Figures 4.4 (a-c), show the variation of three-phase currents at bus-1, 2 and 3 respectively. Differential current, obtained by summation of three-terminal currents, is depicted in Figure 4.4 (d). Figure 4.4 (e) illustrates approximate decomposition for differential current of phase-A alone. Figure 4.4 (f) shows the variation of three-phase fault index with time. It can be observed that the fault index of phase-A is greater than the threshold and those for phase-B and phase-C are less than the threshold. Thus, it is detected as phase-A to ground fault.

Figure 4.5 depicts Fault Index variation of three-phases for different types of faults. Figures 4.5 (a) and 4.5 (b) show the fault index variation for BG and CG faults respectively, in which fault index of faulty phase is greater than the threshold and not for the healthy phases. From Figures 4.5 (c) and 4.5 (f), it is evident that phase-A and phase-B have fault index greater than the threshold, hence they are detected as phase to phase fault. Similarly, Figures 4.5 (d) and 4.5 (g) illustrate the fault index variation for BC and BCG faults respectively, from which it can observed that fault indexes of faulty phases (phase-B & C) are greater than the threshold and not for healthy phase i.e. Phase-A. The fault index variation for AC and ACG faults fault is shown in Figures 4.5 (e) and 4.5 (h), from these figures it is depicted that fault index for phase-A and phase-C are greater than the threshold whereas for phase-B it remains lower than the threshold, hence fault are identified as AC and ACG fault respectively. Figure 4.5 (i) illustrates ABCG fault, since, for all the three-phases, fault indexes are greater than the threshold. Thus, it is detected as three-phase fault.

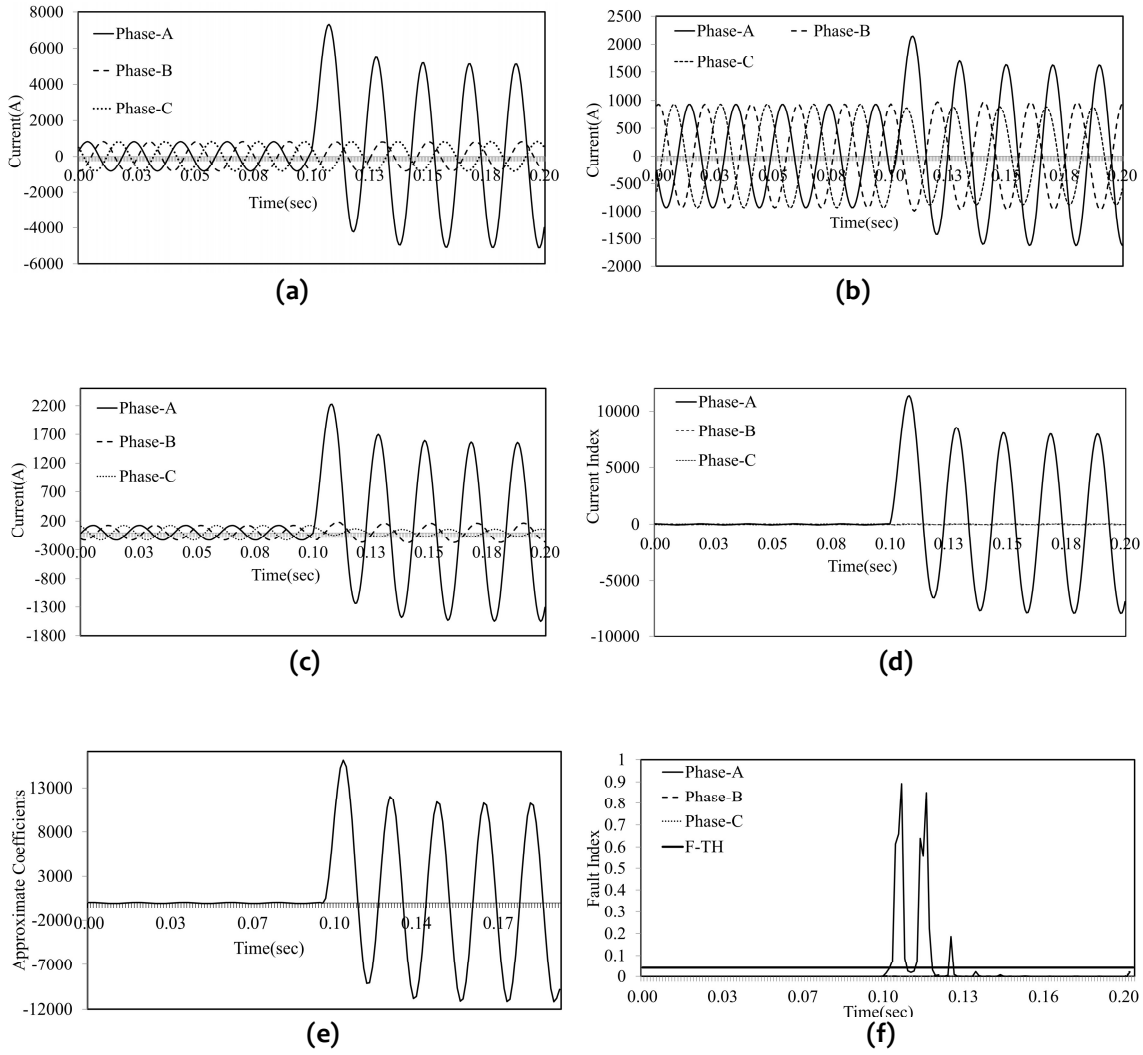

Figure 4.4: Demonstration of AG fault detction: (a) Bus-1 Current Signals, (b) Bus-2 Current Signals, (c) Bus-3 Current Signals, (d) Differential Current, (e) Approximate Coefficients of Phase-A Differential Current, (f) Fault Index variation

It is also evident from Figures 4.5 (c-h) that the discrimination between LLG and LL faults cannot be achieved by fault index alone. To discriminate LLG faults from LL faults, a ground fault index (G-FI) based on zero sequence current is computed. This ground fault index is computed by adding approximate coefficients of zero sequence current over a moving window of quarter cycle length. The same is compared with a ground fault threshold (GF-TH), to discriminate LLG faults from LL faults. From Figure 4.6, it is evident that the ground fault index for LLG fault is greater than the threshold and that of LL fault is lower than the threshold. Thus, LLG faults can be discriminated from LL faults with the help of zero sequence current successfully.

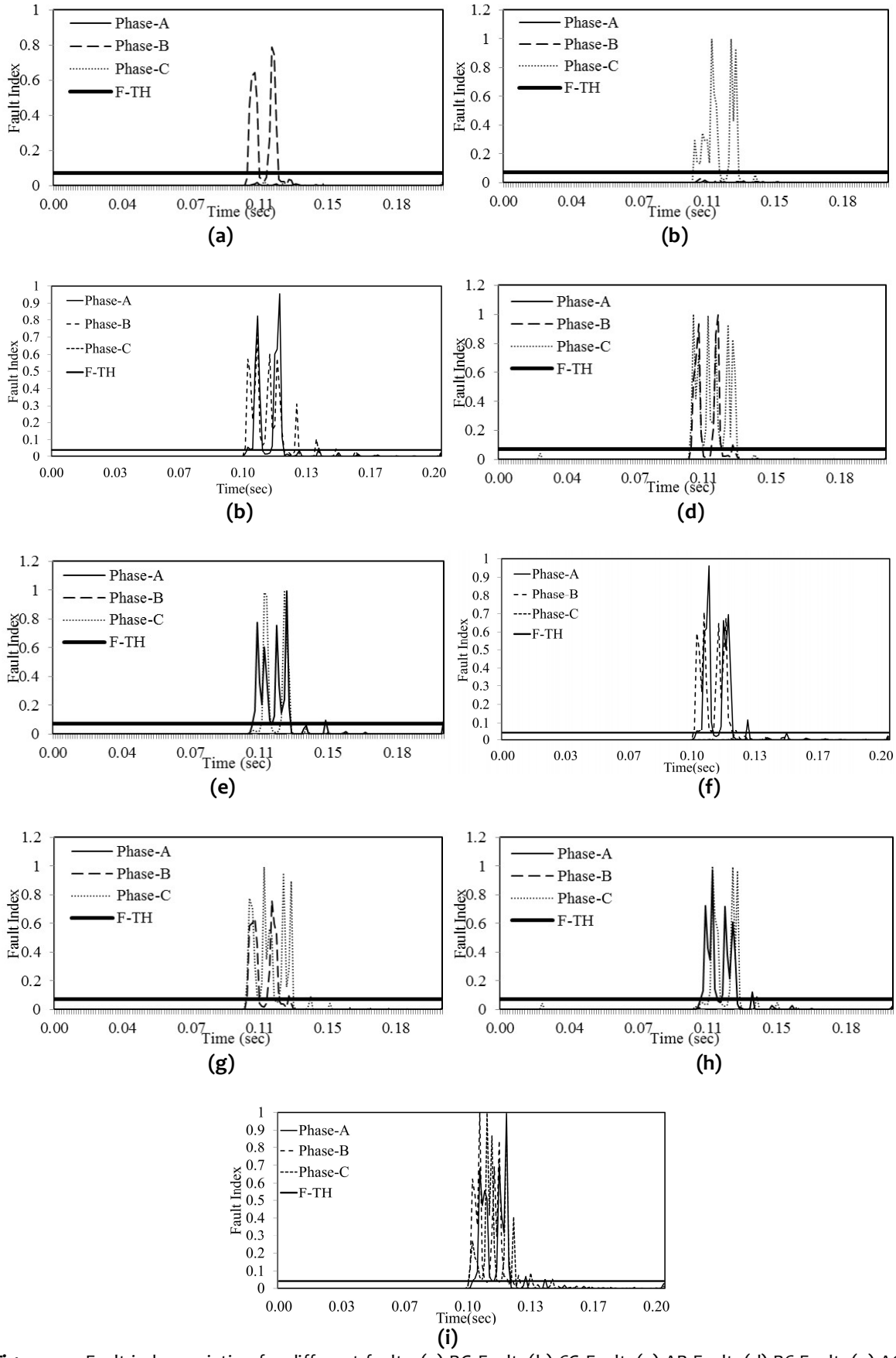

Figure 4.5: Fault index variation for different faults: (a) BG Fault, (b) CG Fault, (c) AB Fault, (d) BC Fault, (e) AC Fault, (f) ABG Fault, (g) BCG Fault, (h) ACG Fault, (i) ABCG Fault

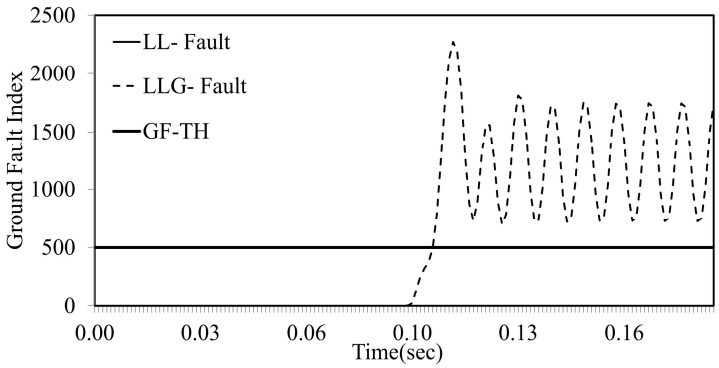

Figure 4.6: Discrimination between LL and LLG Fault

4.5 CASE STUDIES

All the ten types of faults have been considered for the case studies with various fault locations, fault incidence angles, fault impedances and noise contamination to establish the performance of proposed algorithm.

4.5.1 Variation of Fault Location

The post fault current transients are largely dependent on fault locations. Hence, there is a need to test the algorithm for faults at different locations of the transmission system. Figure 4.7 illustrates the variation of fault indexes of three phases at various fault locations. From Figure 4.7 (a), it is evident that fault index of phase-A is always greater than the threshold and those of phase-B and phase-C are less than the threshold for AG fault at different fault locations. Figure 4.7 (b) shows that the fault index of phase-A and phase-C are greater than the threshold and that of phase-B is less than the threshold, for AC faults at all the fault locations. From Figure 4.7 (c), it can be observed that the fault indexes of all the three phases are greater than the threshold for ABCG fault. Thus, proposed algorithm proved to be successful at all the fault locations of line.

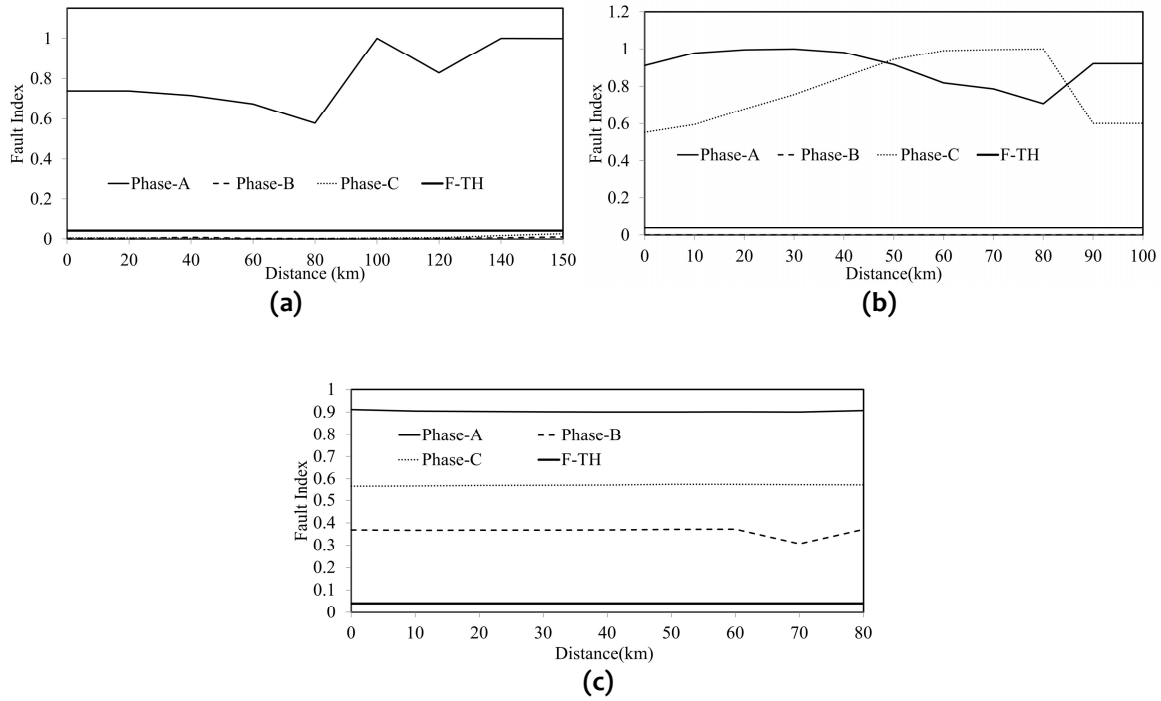

Figure 4.7: Fault Index variation with respect to distance for faults in different sections: (a) AG Fault, (b) AC Fault, (c)ABCG Fault

4.5.2 Effect of Fault incidence Angle

The post fault current transients are also affected by fault incidence angles. Hence, the proposed algorithm is tested for various faults with variations in incidence angle. The angle of incidence has been varied from 0^0 to 180^0 in steps of 30^0 to establish the validity of proposed algorithm. Figure 4.8 shows the fault index variation, for various fault incidence angle for different types of faults. For BG fault, fault index of phase-B is always greater than threshold whereas those of phase-A and phase-C are less than the threshold as shown in Figure 4.8 (a). Figure 4.8 (b) depicts that the fault index of phase-B and phase-C are greater than the threshold at various fault incidence angles for BCG fault. Figure 4.8 (c) illustrates that fault indexes of the three-phases are greater than the threshold in the event of ABCG fault for all the fault incidence angles.

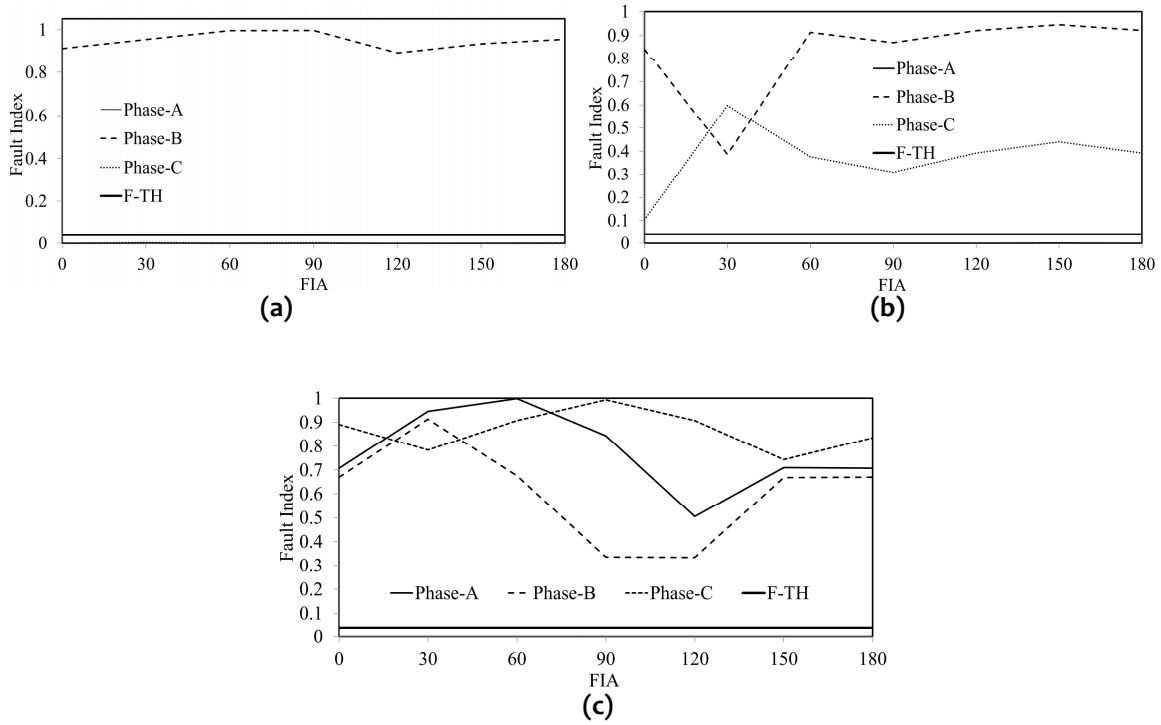

Figure 4.8: Fault Index variation w.r.t. fault incidence angle for faults in different sections: (a) BG Fault, (b) BCG Fault, (c) ABCG Fault

Tables 4.2 to 4.11 demonstrate the successful performance of proposed algorithm for all the types of faults at different locations and with variations in incidence angle.

Table 4.2: Fault Index Variation with different locations and fault incidence angles for AG at 1-P section

FIA	0			30			60			90			120			150		
Location	A	B	C	A	B	C	A	B	C	A	B	C	A	B	C	A	B	C
0	**0.78**	0.04	0.01	**0.79**	0.02	0.01	**0.98**	0.01	0.01	**1.00**	0.01	0.01	**0.88**	0.04	0.03	**0.66**	0.05	0.01
30	**0.73**	0.00	0.00	**0.75**	0.00	0.02	**0.96**	0.00	0.02	**1.00**	0.00	0.03	**0.76**	0.02	0.04	**0.13**	0.00	0.00
60	**0.68**	0.00	0.00	**0.69**	0.00	0.01	**0.92**	0.00	0.02	**0.77**	0.00	0.01	**0.34**	0.00	0.01	**0.05**	0.00	0.00
90	**0.80**	0.00	0.00	**0.89**	0.00	0.00	**0.87**	0.00	0.02	**0.89**	0.00	0.02	**0.12**	0.01	0.04	**0.01**	0.00	0.00
120	**0.95**	0.00	0.00	**1.00**	0.01	0.00	**0.96**	0.00	0.01	**0.82**	0.00	0.00	**0.41**	0.01	0.04	**0.23**	0.00	0.00
150	**0.85**	0.01	0.03	**0.95**	0.02	0.01	**1.00**	0.00	0.02	**0.63**	0.01	0.03	**0.56**	0.01	0.01	**0.67**	0.02	0.00

Table 4.3: Fault Index Variation with different locations and fault incidence angles for AB at 1-P section

FIA	0			30			60			90			120			150		
Location	A	B	C	A	B	C	A	B	C	A	B	C	A	B	C	A	B	C
0	**0.69**	**0.84**	0.00	**0.74**	**0.92**	0.00	**0.97**	**0.96**	0.00	**0.97**	**0.99**	0.00	**0.63**	**0.54**	0.00	**0.29**	**0.57**	0.00
30	**0.91**	**0.86**	0.00	**0.72**	**0.58**	0.00	**0.96**	**0.60**	0.00	**0.99**	**0.79**	0.00	**0.14**	**0.51**	0.00	**0.10**	**0.53**	0.00
60	**0.96**	**0.69**	0.00	**1.00**	**0.86**	0.00	**0.92**	**1.00**	0.00	**0.96**	**0.55**	0.00	**0.48**	**0.55**	0.00	**0.05**	**0.55**	0.00
90	**0.74**	**0.64**	0.00	**1.00**	**0.78**	0.00	**0.98**	**0.76**	0.00	**0.23**	**0.68**	0.00	**0.13**	**0.81**	0.00	**0.01**	**0.94**	0.00
120	**1.00**	**0.95**	0.00	**0.89**	**0.82**	0.00	**0.97**	**0.85**	0.00	**0.52**	**0.85**	0.00	**0.56**	**0.93**	0.00	**0.57**	**0.93**	0.00
150	**0.84**	**0.95**	0.00	**0.92**	**0.70**	0.00	**1.00**	**0.80**	0.00	**0.97**	**0.88**	0.00	**0.98**	**0.97**	0.00	**0.99**	**0.94**	0.00

Table 4.4: Fault Index Variation with different locations and fault incidence angles for ABG at 1-P section

FIA	0			30			60			90			120			150		
Location	A	B	C	A	B	C	A	B	C	A	B	C	A	B	C	A	B	C
0	**0.81**	**0.83**	0.01	**0.85**	**0.92**	0.01	**0.98**	**0.81**	0.01	**1.00**	**0.95**	0.01	**1.00**	**0.57**	0.04	**0.30**	**0.57**	0.01
30	**0.75**	**0.79**	0.04	**0.96**	**0.80**	0.02	**1.00**	**1.00**	0.03	**1.00**	**0.63**	0.03	**0.78**	**0.56**	0.01	**0.11**	**0.57**	0.00
60	**0.69**	**0.96**	0.00	**0.69**	**0.73**	0.00	**0.94**	**0.92**	0.00	**0.92**	**0.60**	0.02	**0.11**	**0.60**	0.02	**0.52**	**0.61**	0.00
90	**1.00**	**0.96**	0.01	**0.95**	**0.81**	0.00	**0.94**	**0.88**	0.00	**0.26**	**0.72**	0.00	**0.02**	**0.84**	0.03	**0.60**	**0.93**	0.00
120	**0.99**	**0.98**	0.01	**0.92**	**0.98**	0.02	**0.98**	**0.96**	0.02	**0.62**	**1.00**	0.03	**0.75**	**0.98**	0.01	**0.90**	**0.81**	0.00
150	**0.98**	**0.99**	0.01	**0.94**	**0.95**	0.01	**1.00**	**0.81**	0.01	**0.72**	**0.75**	0.01	**0.75**	**0.92**	0.00	**0.79**	**0.70**	0.01

Table 4.5: Fault Index Variation with different locations and fault incidence angles for BG at 2-P section

FIA	0			30			60			90			120			150		
Location	A	B	C	A	B	C	A	B	C	A	B	C	A	B	C	A	B	C
0	0.03	**0.95**	0.02	0.07	**0.59**	0.01	0.03	**0.86**	0.01	0.01	**0.99**	0.06	0.00	**0.97**	0.03	0.00	**0.70**	0.00
20	0.00	**0.94**	0.02	0.02	**0.53**	0.02	0.01	**0.80**	0.01	0.00	**0.97**	0.03	0.00	**0.93**	0.01	0.00	**0.66**	0.00
40	0.01	**0.92**	0.01	0.02	**0.55**	0.07	0.02	**0.66**	0.00	0.00	**0.91**	0.03	0.00	**0.82**	0.01	0.00	**0.75**	0.00
60	0.03	**0.98**	0.06	0.01	**0.72**	0.06	0.03	**0.57**	0.01	0.00	**0.79**	0.00	0.00	**0.64**	0.01	0.00	**0.96**	0.00
80	0.02	**0.99**	0.09	0.06	**0.86**	0.01	0.01	**0.53**	0.03	0.00	**0.67**	0.02	0.00	**0.85**	0.02	0.00	**0.93**	0.00
100	0.02	**0.85**	0.01	0.03	**1.00**	0.01	0.03	**0.91**	0.03	0.00	**0.57**	0.03	0.00	**0.64**	0.34	0.00	**0.62**	0.03

Table 4.6: Fault Index Variation with different locations and fault incidence angles for BC at 2-P section

FIA	0			30			60			90			120			150		
Location	A	B	C	A	B	C	A	B	C	A	B	C	A	B	C	A	B	C
0	0.00	**0.98**	**1.00**	0.00	**0.72**	**0.87**	0.00	**0.61**	**0.87**	0.00	**0.67**	**0.96**	0.00	**1.00**	**0.95**	0.00	**0.94**	**0.38**
20	0.00	**0.91**	**0.97**	0.00	**0.72**	**0.87**	0.00	**0.63**	**0.87**	0.00	**0.78**	**0.98**	0.00	**0.98**	**0.94**	0.00	**1.00**	**0.39**
40	0.00	**0.98**	**0.99**	0.00	**0.79**	**0.87**	0.00	**0.72**	**0.86**	0.00	**0.94**	**1.00**	0.00	**0.89**	**0.91**	0.00	**0.98**	**0.41**
60	0.00	**1.00**	**1.00**	0.00	**0.89**	**0.88**	0.00	**0.84**	**0.87**	0.00	**0.98**	**0.95**	0.00	**0.73**	**0.87**	0.00	**0.89**	**0.42**
80	0.00	**0.99**	**1.00**	0.00	**0.96**	**0.90**	0.00	**0.94**	**0.91**	0.00	**0.70**	**0.86**	0.00	**0.62**	**0.82**	0.00	**0.74**	**0.45**
100	0.00	**0.99**	**0.90**	0.00	**1.00**	**0.86**	0.00	**0.99**	**0.93**	0.00	**0.61**	**0.86**	0.00	**1.00**	**1.00**	0.00	**0.61**	**0.47**

Table 4.7: Fault Index Variation with different locations and fault incidence angles for BCG at 2-P section

FIA	0			30			60			90			120			150		
Location	A	B	C	A	B	C	A	B	C	A	B	C	A	B	C	A	B	C
0	0.04	**0.92**	**0.93**	0.05	**0.92**	**0.93**	0.01	**0.98**	**0.92**	0.01	**1.00**	**0.92**	0.00	**0.86**	**0.91**	0.00	**0.89**	**0.39**
20	0.04	**0.91**	**0.92**	0.01	**0.88**	**0.92**	0.01	**1.00**	**0.92**	0.02	**0.99**	**0.92**	0.00	**0.92**	**0.89**	0.00	**0.98**	**0.40**
40	0.03	**0.89**	**0.92**	0.03	**0.81**	**0.91**	0.00	**0.99**	**0.91**	0.01	**0.92**	**0.92**	0.00	**1.00**	**0.87**	0.00	**1.00**	**0.41**
60	0.03	**0.88**	**0.92**	0.03	**0.74**	**0.92**	0.01	**0.95**	**0.91**	0.01	**0.81**	**0.92**	0.00	**0.92**	**0.84**	0.00	**0.93**	**0.43**
80	0.00	**0.86**	**0.92**	0.04	**0.91**	**0.92**	0.01	**0.91**	**0.95**	0.00	**0.69**	**0.92**	0.00	**0.70**	**0.80**	0.00	**0.77**	**0.45**
100	0.01	**0.96**	**0.99**	0.01	**1.00**	**0.99**	0.01	**0.97**	**0.94**	0.02	**0.96**	**0.94**	0.01	**0.54**	**0.89**	0.01	**0.61**	**0.47**

Table 4.8: Fault Index Variation with different locations and fault incidence angles for CG at 3-P section

FIA	0			30			60			90			120			150		
Location	A	B	C	A	B	C	A	B	C	A	B	C	A	B	C	A	B	C
0	0.01	0.05	**0.95**	0.03	0.04	**0.95**	0.03	0.04	**0.95**	0.03	0.05	**0.95**	0.01	0.01	**0.82**	0.01	0.05	**0.44**
20	0.07	0.01	**0.95**	0.01	0.02	**0.95**	0.01	0.09	**0.95**	0.01	0.04	**0.95**	0.00	0.02	**0.87**	0.00	0.02	**0.41**
40	0.01	0.03	**0.96**	0.01	0.03	**1.00**	0.05	0.02	**0.99**	0.01	0.04	**0.95**	0.00	0.03	**0.92**	0.00	0.04	**0.38**
60	0.01	0.01	**1.00**	0.01	0.01	**0.94**	0.02	0.01	**0.95**	0.06	0.00	**0.95**	0.00	0.01	**0.94**	0.00	0.28	**0.36**
80	0.01	0.01	**0.97**	0.00	0.02	**0.94**	0.02	0.01	**0.94**	0.02	0.01	**0.94**	0.01	0.05	**0.96**	0.01	0.02	**0.36**

Table 4.9: Fault Index Variation with different locations and fault incidence angles for AC at 3-P section

FIA	0			30			60			90			120			150		
Location	A	B	C	A	B	C	A	B	C	A	B	C	A	B	C	A	B	C
0	**0.92**	0.00	**0.98**	**1.00**	0.00	**1.00**	**1.00**	0.00	**0.98**	**0.86**	0.00	**0.98**	**0.69**	0.00	**0.83**	**0.62**	0.00	**0.70**
20	**0.96**	0.00	**0.98**	**0.97**	0.00	**0.98**	**1.00**	0.00	**0.98**	**0.83**	0.00	**0.98**	**0.67**	0.00	**0.86**	**0.52**	0.00	**0.57**
40	**0.96**	0.00	**0.98**	**0.97**	0.00	**0.98**	**1.00**	0.00	**0.98**	**0.80**	0.00	**0.98**	**0.61**	0.00	**0.89**	**0.45**	0.00	**0.47**
60	**0.94**	0.00	**0.98**	**0.95**	0.00	**0.98**	**1.00**	0.00	**0.98**	**0.76**	0.00	**0.98**	**0.55**	0.00	**0.91**	**0.40**	0.00	**0.41**
80	**0.95**	0.00	**0.98**	**0.95**	0.00	**0.98**	**1.00**	0.00	**0.98**	**0.75**	0.00	**0.97**	**0.49**	0.00	**0.93**	**0.42**	0.00	**0.42**

Table 4.10: Fault Index Variation with different locations and fault incidence angles for ACG at 3-P section

FIA	0			30			60			90			120			150		
Location	A	B	C	A	B	C	A	B	C	A	B	C	A	B	C	A	B	C
0	**0.93**	0.01	**0.95**	**0.96**	1.00	**0.95**	**0.99**	0.01	**0.95**	**1.00**	0.01	**0.95**	**0.98**	0.02	**0.80**	**0.99**	0.01	**0.44**
20	**0.93**	0.01	**0.96**	**0.88**	0.63	**0.96**	**1.00**	0.02	**0.96**	**0.83**	0.04	**0.96**	**0.54**	0.04	**0.83**	**0.61**	0.04	**0.41**
40	**0.87**	0.04	**0.96**	**0.99**	0.21	**0.96**	**1.00**	0.02	**0.96**	**0.79**	0.02	**0.96**	**0.77**	0.02	**0.86**	**0.85**	0.02	**0.39**
60	**0.88**	0.14	**0.96**	**1.00**	0.16	**0.96**	**1.00**	0.01	**0.96**	**0.76**	0.02	**0.96**	**0.88**	0.02	**0.90**	**0.96**	0.01	**0.38**
80	**0.92**	0.13	**0.96**	**0.96**	0.14	**0.96**	**1.00**	0.01	**0.96**	**0.73**	0.04	**0.96**	**0.95**	0.04	**0.90**	**1.00**	0.02	**0.37**

4.5.3 Performance with High Impedance Faults

Faults with high impedance, affect the sensitivity of protection scheme and thus are difficult to detect due to low magnitude of fault currents. Thus, there is a need to test the proposed algorithm for various fault impedances to establish its performance. The proposed algorithm has been tested with fault impedances of 0-100 Ω. Figures 4.9-4.10 show the variation of fault index for three phases for different types of faults, with a fault impedance of 100 Ω. Figure 4.9 (a) depicts that for phase-A (faulty phase) fault index is greater than the threshold

and not for phase-B and phase-C (healthy phase), hence detects the fault as phase to ground (AG) fault. Figures 4.9 (b) and 4.9 (c) show the fault index variation for BG and CG faults respectively, in which fault index of faulty phase is greater than the threshold and not for the healthy phases. Figures 4.9 (d) and 4.10 (c) depict the variation of three-phase fault indexes for AB and ABG faults respectively. Form these figures, it is evident that phase-A and phase-B have fault index greater than the threshold. Similarly, Figures 4.10 (a) and 4.10 (d) illustrate the fault index variation for BC and BCG faults respectively, from which it can observed that fault indexes of faulty phases (phase-B & C) are greater than the threshold and not for healthy phase i.e. Phase-A. The fault index variation for AC and ACG faults is shown in Figures 4.10 (b) and 4.10 (e), from these figures it is depicted that fault index for phase-A and phase-C are greater than the threshold whereas for phase-B it remains lower than the threshold, hence fault are identified as AC and ACG fault respectively. Figure 4.10 (f) shows that for all the three phases, fault index is greater than the threshold, hence it is detected as three phase to ground (ABCG) fault. Thus, it is evident that the fault impedance has no effect on proposed algorithm.

Table 4.11: Fault Index Variation with different locations and fault incidence angles for ABCG at 3-P section

FIA	0			30			60			90			120			150		
Location	A	B	C	A	B	C	A	B	C	A	B	C	A	B	C	A	B	C
0	**0.87**	**0.88**	**0.95**	**0.79**	**0.59**	**0.95**	**0.98**	**0.86**	**0.95**	**1.00**	**0.99**	**0.95**	**0.88**	**0.97**	**0.82**	**0.66**	**0.70**	**0.44**
20	**0.93**	**0.89**	**0.95**	**0.75**	**0.53**	**0.95**	**0.96**	**0.80**	**0.95**	**1.00**	**0.97**	**0.95**	**0.76**	**0.93**	**0.87**	**0.13**	**0.66**	**0.41**
40	**1.00**	**0.90**	**0.95**	**0.69**	**0.55**	**1.00**	**0.92**	**0.66**	**0.99**	**0.77**	**0.91**	**0.95**	**0.34**	**0.82**	**0.92**	**0.05**	**0.75**	**0.38**
60	**0.93**	**0.91**	**0.95**	**0.89**	**0.72**	**0.94**	**0.87**	**0.57**	**0.95**	**0.89**	**0.79**	**0.95**	**0.12**	**0.64**	**0.94**	**0.01**	**0.96**	**0.36**
80	**0.84**	**0.92**	**0.99**	**1.00**	**0.86**	**0.94**	**0.96**	**0.53**	**0.94**	**0.82**	**0.67**	**0.94**	**0.41**	**0.85**	**0.96**	**0.23**	**0.93**	**0.36**

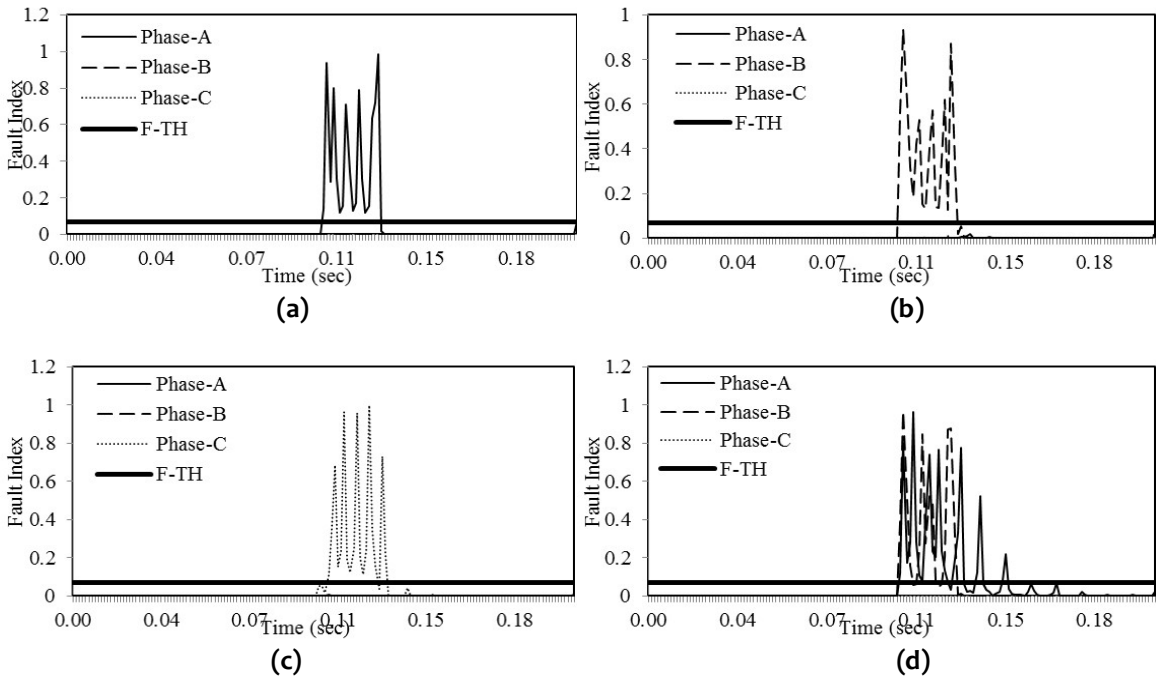

Figure 4.9: Fault index variation w.r.t time for high impedance faults: (a) AG Fault, (b) BG Fault, (c) CG Fault, (d) AB Fault,

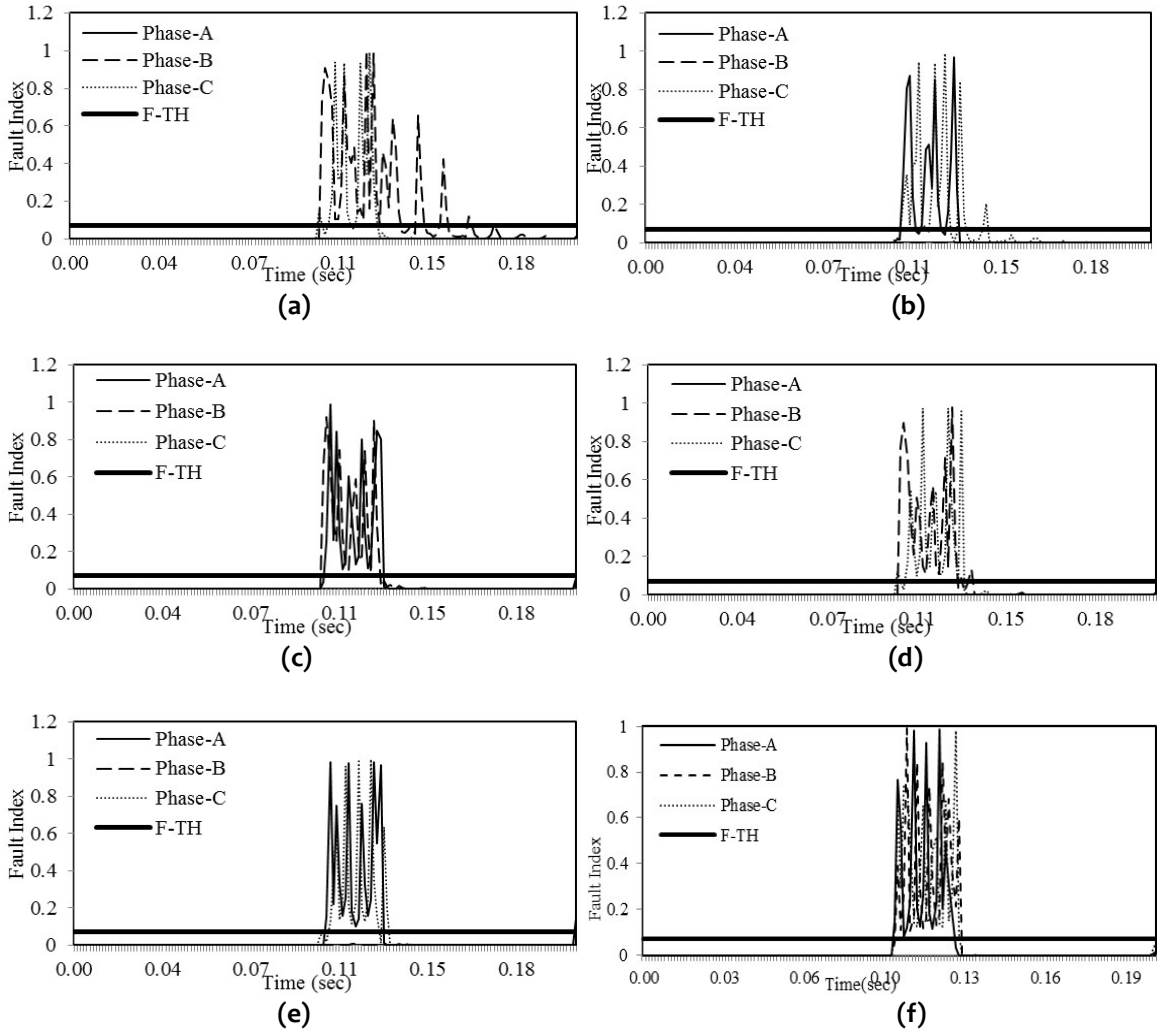

Figure 4.10: Fault index variation w.r.t time for high impedance faults: (a) BC Fault, (b) AC Fault, (c) ABG Fault, (d) BCG Fault, (e) ACG Fault, (f) ABCG Fault

4.5.4 Performance in Noisy Environment

To examine the noise influence on proposed algorithm, the current signals are contaminated with different levels of noise. Figure 4.10 depicts variation of three-phase fault index for different types of faults, with 10dB and 20dB white Gaussian noise. Figure 4.11(a) depicts variation of fault index for AG fault. The fault index of phase-A is greater than the threshold and that of other phases is less than the threshold, thus illustrating AG fault. Figure 4.11(b) illustrates that for phase-A and phase-B, fault index is greater than the threshold and not for phase-C, and hence the fault is detected as ABG fault. Figure 4.11 (c) shows that for all the three phases, fault index is greater than the threshold. Hence it is detected as ABCG fault. Thus, it is evident that presence of noise in the current signals has no effect on proposed algorithm.

4.5.5 Effect of Loading

The proposed algorithm has been tested with load switching. It has been observed that for 10% and 20% load switching, the maximum values of fault index for phase-A, phase-B and phase-C are well below the threshold value. Fig 4.12 (a) and 4.12 (b) shows the effect of 10 % and 20 % loading for the proposed algorithm.

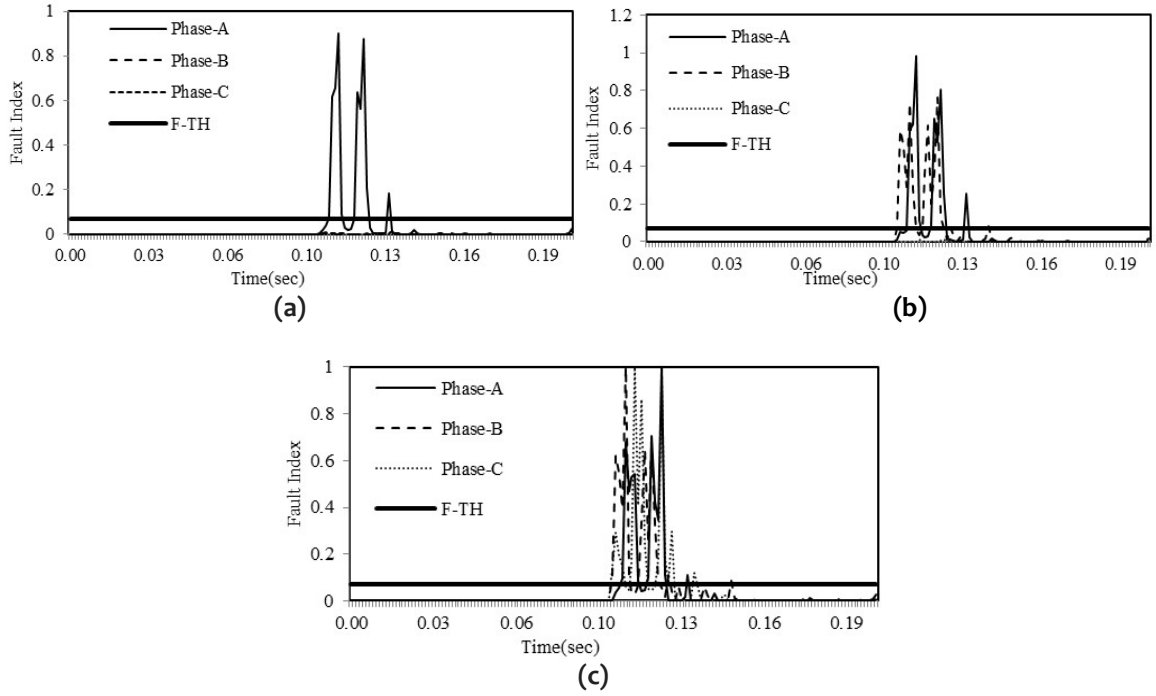

Figure 4.11: Fault index variation w.r.t time, for noise effects: (a) AG Fault, (b) ABG Fault, (c) ABCG Fault

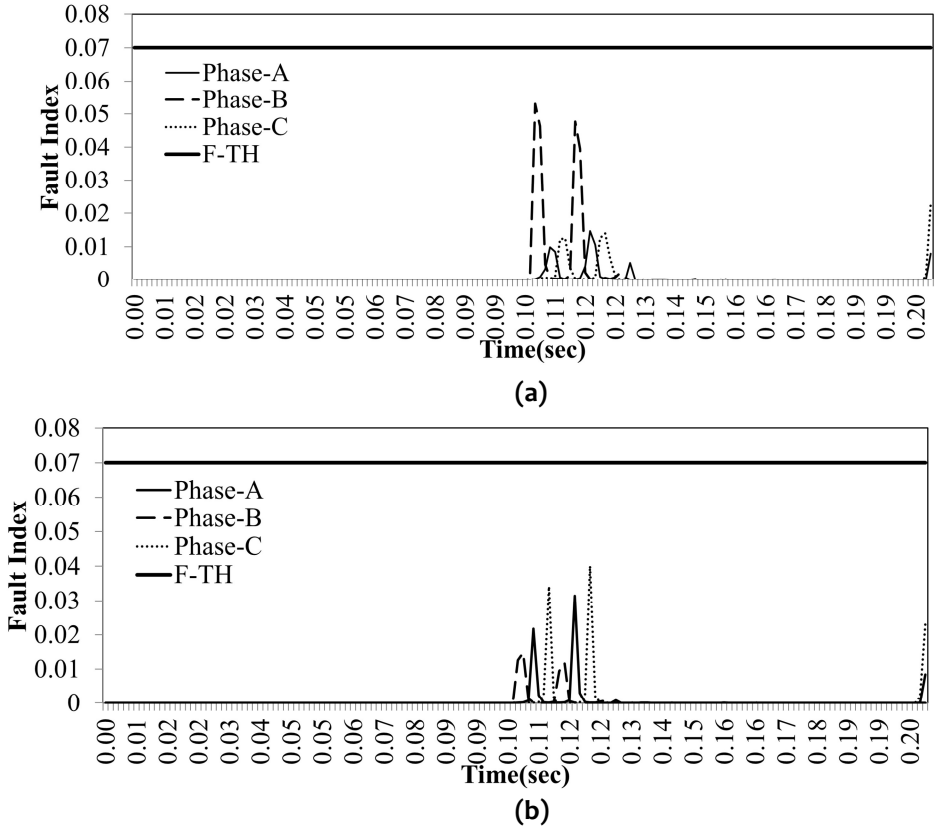

Figure 3.13: Variation of fault index with time for effect of loading; (a) 10% loading, (b) 20 % loading

4.6 DETECTION OF FAULTY SECTION AND ESTIMATION OF FAULT LOCATION

For fault location and detection of faulty section, an Artificial Neural Network is used at each bus. The approximation coefficients, obtained from post-fault voltage and current signals over a quarter cycle from the respective buses are fed as inputs to feed-forward neural network. Artificial Neural Network is trained to yield fault location in kms, as output from each bus. A

multi-layer perceptron model with Levenberg-Marquardt optimization method has been adopted for this purpose. Figure 4.13 depicts structure of proposed ANN for the fault location. The details related to ANN structure are presented in Table 4.11.

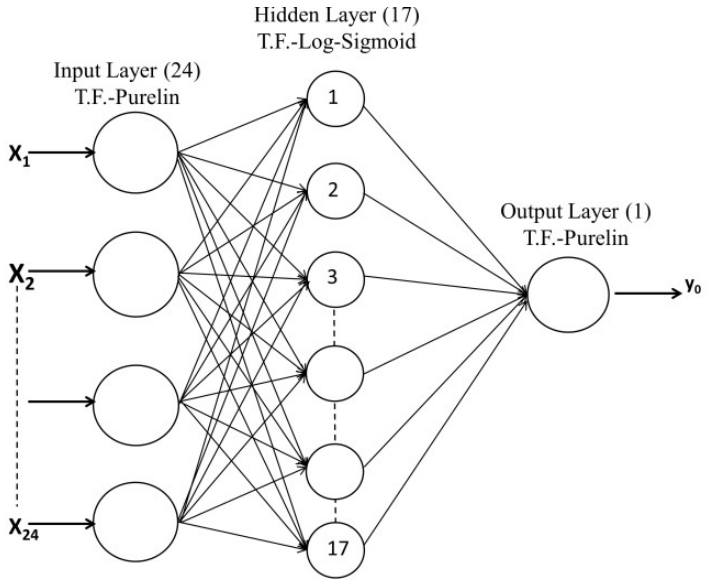

Figure 4.13: ANN Architecture

The algorithm for identification of faulty section is as follows:

a) If $Di_1 < L_{1P}$ and $Di_2 > L_{2P}$ and $Di_3 > L_{3P}$, then the fault is in section 1-P.
b) If $Di_2 < L_{2P}$ and $Di_1 > L_{1P}$ and $Di_3 > L_{3P}$, then the fault is in section 2-P.
c) If $Di_3 < L_{3P}$ and $Di_1 > L_{1P}$ and $Di_2 > L_{2P}$, then the fault is in section 3-P.

where, Di_1 = Fault Location from bus-1; Di_2 = Fault Location from bus-2; Di_3 = Fault Location from bus-3; L_{1P}= Length of the Section 1-P; L_{2P}= Length of the Section 2-P; L_{3P}= Length of the Section 3-P. The error in determination of fault location is evaluated as follows:

$$\%Error = \frac{|NNDis\tan ce - ActualDis\tan ce|}{L} * 100$$

Table 4.12: Details of ANN

ANN Layers	Number of Neurons	Transfer Function
Input	24	Purelin
Hidden	17	Log-sigmoid
Output	1	Purelin

Tables 4.13 to 4.14, show the performance of ANN for AG and ABG faults at Section 1-P. It is observed from theses tables for all the faults and all the locations $D_1 < L_{1P}$ and $D_2 > L_{2P}$ and $D_3 > L_{3P}$, which verifies that the fault is in section 1-P. From Tables 4.15 to 4.16, fault section and location identification is done for BG and BC faults, respectively. It is verified that for different faults and locations, $D_2 < L_{2P}$ and $D_1 > L_{1P}$ and $D_3 > L_{3P}$, is verified for fault in section 2-P. The Tables 4.17 to 4.18, show the detection of faulty section and estimation of fault location using ANN for CG and ABCG faults at various locations. It can be observed that $D_3 < L_{3P}$ and $D_1 > L_{1P}$ and $D_2 > L_{2P}$, which establishes that the faulty section is 3-P.

Thus, these results establish that the proposed algorithm is found to be successful to identify the faulty section and to locate the faults with an average and maximum error of 0.82% and 3.06% respectively.

Table 4.13: For Fault At Section 1-P (For AG Fault)

S.No	Actual Distance from bus-1 (kms)	ANN Distance			% Error
		Di_1	Di_2	Di_3	
1	15	12.82	227.39	216.80	0.87
2	45	50.87	201.41	188.32	2.35
3	85	82.84	170.44	141.28	0.86
4	125	123.52	125.44	118.92	0.59
5	145	144.88	101.47	85.64	0.05

Table 4.14: For Fault At Section 1-P (For ABG Fault)

S.No	Actual Distance from bus-1 (kms)	ANN Distance			% Error
		Di_1	Di_2	Di_3	
1	15	16.08	226.02	212.06	0.43
2	45	45.48	205.97	186.69	0.20
3	85	87.75	165.17	141.60	0.90
4	125	123.85	129.90	107.31	0.46
5	145	139.38	109.81	85.73	2.25

Table 4.15: For Fault At Section 2-P (For BG Fault)

S.No	Actual Distance from bus-2 (kms)	ANN Distance			% Error
		Di_1	Di_2	Di_3	
1	15	234.04	15.91	169.34	0.37
2	45	204.69	46.46	137.49	0.58
3	85	169.72	88.59	94.50	1.43
4	95	148.25	88.75	84.57	2.50

Table 4.16: For Fault At Section 2-P (For BC Fault)

S.No	Actual Distance from bus-2 (kms)	ANN Distance			% Error
		Di_1	Di_2	Di_3	
1	15	224.90	15.09	162.04	0.04
2	45	212.25	45.86	134.24	0.34
3	85	164.31	86.74	96.21	0.70
4	95	154.91	92.96	85.24	0.82

Table 4.17: For Fault At Section 3-P (For CG Fault)

S.No	Actual Distance from bus-3 (kms)	ANN Distance			% Error
		Di_1	Di_2	Di_3	
1	15	225.32	165.25	14.75	0.10
2	35	194.93	160.96	36.19	0.48
3	65	169.62	114.86	68.75	1.50
4	75	159.54	101.85	73.75	0.50

Table 4.18: For Fault At Section 3-P (For ABCG Fault)

S.No	Actual Distance from bus-3 (kms)	ANN Distance			% Error
		Di_1	Di_2	Di_3	
1	15	211.33	164.99	11.81	1.28
2	35	194.97	140.97	36.76	0.70
3	65	168.24	115.56	64.53	0.19
4	75	159.46	107.32	70.53	1.79

4.7 GENERALIZATION OF ALGORITHM

The proposed algorithm can be extended for n-terminal transmission system. As a part of generalization, the algorithm has been applied to a 5-bus system as shown in Figure 4.14 and whose parameters are given in Table 4.19.

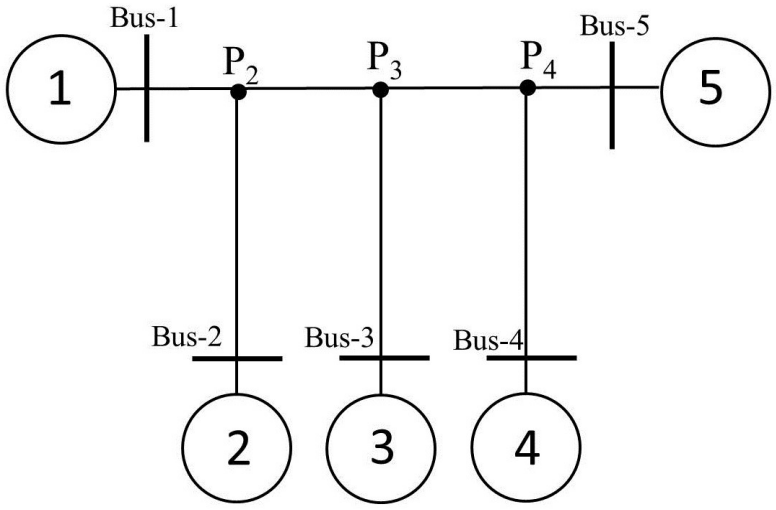

Figure 4.14: Five-terminal transmission system

4.7.1 Fault Detection and Fault Classification

Figure 4.15 depicts fault detection and fault classification for different types of faults on 5-terminal system.

Table 4.19: Parameters for 5- terminal system

Source Voltage (kV)		Vo_1	Vo_2	Vo_3	Vo_4	Vo_5
		$345\angle 0^0$	$345\angle 5^0$	$345\angle 15^0$	$345\angle 20^0$	$345\angle 30^0$
Source Imp. (Ω)	Positive Sequence	Z_{11}	Z_{21}	Z_{31}	Z_{41}	Z_{51}
		0.238+j6.19	0.42+j5.95	0.155+j5.95	0.238+j5.72	0.238+j5.72
	Zero Sequence	Z_{10}	Z_{20}	Z_{30}	Z_{40}	Z_{50}
		0.833+j5.12	1.785+j7.54	1.178+j5.78	2.74+j10	2.74+j10
Line Imp. (Ω/km)	Positive Sequence	0.065+j0.435				
	Zero Sequence	0.455+j1.21				

Line Lengths (km)	Bus-1 to P_2	Bus 2 to P_2	Bus-3 to P_3	Bus-4 to P_4	Bus-5 to P_4	P_2 to P_3	P_3 to P_4
	100	80	180	100	160	100	100

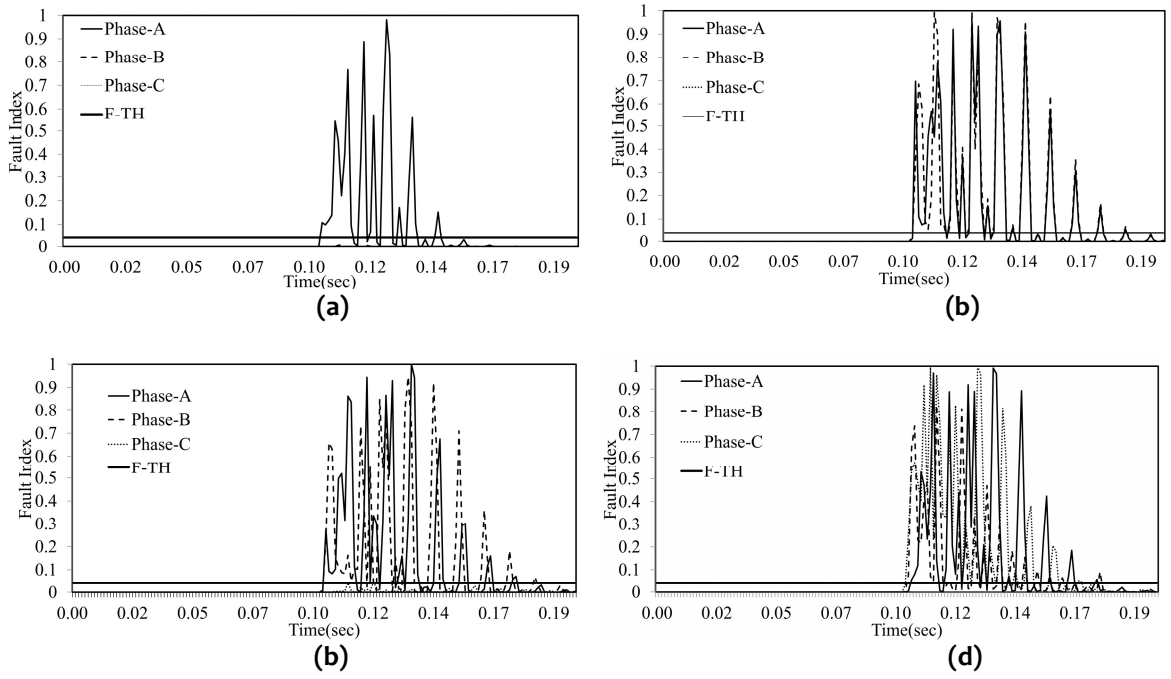

Figure 4.15: Fault Index variation with time for different faults: (a) AG Fault in section 5-P_4, (b) AB Fault in section 4-P_4, (c) ABG Fault in section 2-P_2 and (d) ABCG Fault in section 1-P_2

4.7.2 Detection of Faulty Section and Location of Fault

Subsequent to fault detection, fault location and faulty section identification are carried out with the help of ANN at each bus. These ANNs are fed from approximate decomposition of current and voltage signals of a quarter cycle.

The results of Table 4.20 also establishes the applicability of proposed scheme for faulty section identification, hence it can be generalized as follows:

a) If $Di_1 < L_1$ and $Di_2 > L_2$ and $Di_3 > L_3$ and $Di_4 > L_4$ and $Di_5 > L_5$, then fault is in section 1-P_2.
b) If $Di_2 < L_2$ and $Di_1 > L_1$ and $Di_3 > L_3$ and $Di_4 > L_4$ and $Di_5 > L_5$, then fault is in section 2-P_2.
c) If $Di_3 < L_3$ and $Di_1 > L_1$ and $Di_2 > L_2$ and $Di_4 > L_4$ and $Di_5 > L_5$, then fault is in section 3-P_3.
d) If $Di_4 < L_4$ and $Di_1 > L_1$ and $Di_2 > L_2$ and $Di_3 > L_3$ and $Di_5 > L_5$, then fault is in section 4-P_4.
e) If $Di_5 < L_5$ and $Di_1 > L_1$ and $Di_2 > L_2$ and $Di_3 > L_3$ and $Di_4 > L_4$, then fault is in section 5-P_4.
f) If $Di_1 > L_1$ and $Di_2 > L_2$ and $Di_3 > L_3$ and $Di_4 > L_4$ and $Di_5 > L_5$, and $Di_1 < L_{123}$, then fault is in section P_2- P_3.
g) If $Di_1 > L_1$ and $Di_2 > L_2$ and $Di_3 > L_3$ and $Di_4 > L_4$ and $Di_5 > L_5$,and $Di_1 < L_{134}$, then fault is in section P_3- P_4

where, Di_1= ANN Fault Location from Bus-1; Di_2= ANN Fault Location from Bus-2; Di_3= ANN Fault Location from Bus-3; Di_4= ANN Fault Location from Bus-4; Di_5= ANN Fault Location from Bus-5; L_1= Length of Section 1-P_2; L_2= Length of Section 2-P_2; L_3= Length of Section 3-P_3; L_4= Length of Section 4-P_4; L_5= Length of Section 5-P_4 ; L_{23}= Length of Section between P_2 and P_3; L_{34}= Length of Section between P_3 and P_4; L_{123}= L_1+ L_{23} & L_{134}= L_1+ L_{34}.

The performance of proposed algorithm for estimation of fault location is presented in Table-4.20, for various faults at different fault locations. The proposed algorithm has been successful in locating the faults with an average error of 0.32%.

4.8 CONCLUSION

A wavelet-alienation based algorithm, for protection of multi-terminal transmission lines, has been proposed. The three-phase currents have been utilized for detection and classification of faults, whereas three-phase voltages and currents decomposed by wavelet transform are utilized to estimate the faulty section to a fair degree of accuracy using artificial

neural network. Based on simulation results the proposed has been successful in detection, classification and locating various types of faults in all the sections of multi-terminal transmission systems. The case studies establish that the proposed algorithm is not affected by fault type, fault location, fault incidence angle, noise contamination and fault impedance.

Table 4.20 : Performance of ANN for locating faults in five-terminal system

S.No.	Fault Section and Fault Location	Fault Type	ANN Fault Locations					% Error
			D_1	D_2	D_3	D_4	D_5	
1	(1-P_2) & 15 kms from Bus-1	ABCG	15.01	167.30	363.94	382.12	440.68	0.00
2	(1-P_2) & 35 kms from Bus-1	ABCG	36.96	145.19	347.61	366.32	425.68	0.43
3	(1-P_2) & 55 kms from Bus-1	ABCG	54.93	124.67	323.07	346.61	407.45	0.02
4	(1-P_2) & 75 kms from Bus-1	ABCG	77.56	105.36	308.18	329.28	387.01	0.56
5	(2-P_2) & 15 kms from Bus-2	ABG	165.67	18.97	343.51	364.09	424.88	0.86
6	(2-P_2) & 35 kms from Bus-2	ABG	141.92	35.05	323.75	346.10	409.16	0.01
7	(2-P_2) & 55 kms from Bus-2	ABG	124.86	55.02	305.14	326.19	383.52	0.00
8	(2-P_2) & 75 kms from Bus-2	ABG	104.98	72.00	283.35	307.10	364.50	0.65
9	(3-P_3) & 55 kms from Bus-3	BC	326.33	307.12	54.85	324.83	384.92	0.03
10	(3-P_3) & 95 kms from Bus-3	BC	284.55	265.29	98.94	285.94	345.35	0.86
11	(3-P_3) & 135 kms from Bus-3	BC	247.89	228.30	134.84	244.31	306.87	0.03
12	(3-P_3) & 175 kms from Bus-3	BC	204.86	186.71	176.28	204.81	265.66	0.28
13	(4-P_4) & 15 kms from Bus-4	ACG	383.12	360.68	365.89	15.07	246.74	0.02
14	(4-P_4) & 35 kms from Bus-4	ACG	368.41	341.98	344.12	31.09	227.06	0.85
15	(4-P_4) & 55 kms from Bus-4	ACG	345.34	326.02	322.02	56.80	205.25	0.39
16	(4-P_4) & 75 kms from Bus-4	ACG	322.78	305.77	304.14	74.95	185.44	0.01
17	(5-P_4) & 15 kms from Bus-5	AG	443.12	425.60	423.14	244.78	15.21	0.05
18	(5-P_4) & 55 kms from Bus-5	AG	406.50	387.31	386.26	203.65	57.08	0.45
19	(5-P_4) & 95 kms from Bus-5	AG	365.82	346.21	344.65	154.23	95.02	0.00
20	(5-P_4) &135 kms from Bus-5	AG	324.69	305.43	305.98	125.83	132.87	0.46
21	(P_2-P_3) &115 kms from Bus-1	BG	111.02	96.23	265.48	284.12	344.89	0.27
22	(P_2-P_3) &135 kms from Bus-1	BG	136.01	118.69	247.63	263.26	327.35	0.80
23	(P_2-P_3) &155 kms from Bus-1	BG	155.07	136.25	228.91	245.23	308.25	0.27
24	(P_2-P_3) &175 kms from Bus-1	BG	174.98	154.87	203.64	221.45	282.55	0.03
25	(P_3-P_4) & 215 kms from Bus-1	CG	214.97	198.56	198.56	195.64	247.89	0.01
26	(P_3-P_4) & 235 kms from Bus-1	CG	238.84	214.36	216.34	217.36	223.69	0.83
27	(P_3-P_4) & 255 kms from Bus-1	CG	252.17	233.47	236.56	238.95	204.91	0.62
28	(P_3-P_4) & 275 kms from Bus-1	CG	275.12	257.16	255.89	256.38	184.76	0.03